

Elastic Moduli of Diamond

H. J. MCSKIMIN AND W. L. BOND
Bell Telephone Laboratories, Murray Hill, New Jersey

(Received September 19, 1956)

The adiabatic elastic moduli of single crystal diamond have been determined by means of ultrasonic waves in the frequency range 20–200 Mc/sec. c_{12} is much lower and c_{44} much higher than respective values reported in the literature. In units of 10^{12} dynes per cm^2 , the newly determined values are: $c_{11}=10.76$; $c_{12}=1.250$; $c_{44}=5.758$. A critical analysis of uncertainties and a comparison with results obtained by others are made.

I. INTRODUCTION

ALTHOUGH diamond has been a much studied material, few references are to be found in the literature pertaining to the measurement of the elastic moduli. Bhagavantam and Bhimasenachar¹ list values obtained by an ultrasonic “wedge” method, while Prince and Wooster² have used a technique involving measurement of the intensity of diffuse x-rays thermally scattered from diamond. It is to be noted that there is considerable disagreement between the two sets of data. In view of the importance of having available accurate values for use in theoretical studies, it was felt desirable to redetermine the elastic constants using a refinement of a technique previously used and described.³ In the following sections, the results of this study will be detailed along with a critical analysis of the possible uncertainties.

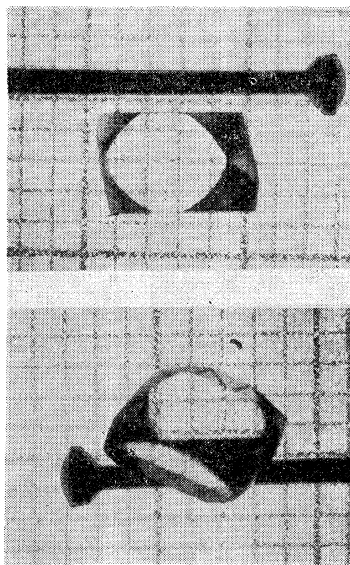


FIG. 1. Diamond No. 1 on millimeter paper background with common straight pin for comparison.

¹ S. Bhagavantam and J. Bhimasenachar, Proc. Roy. Soc. (London) **A187**, 381 (1946).

² E. Prince and W. A. Wooster, Acta Cryst. **6**, 450 (1953).

³ H. J. McSkimin, J. Appl. Phys. **24**, 988 (1953).

II. DESCRIPTION OF SPECIMENS USED

The diamonds used were obtained from J. K. Smith and Sons. They were of a pale yellow cast but quite transparent. One weighed 1.12 carats, the other 1.28 carats before cutting. They were unusual only in that they were natural dodecahedra (with rounded faces), not the more usual octahedra. Figure 1 shows the No. 1 specimen after two sets of faces were cut. Thickness in the $[110]$ direction was measured as 0.32410 cm, and in the $[001]$ direction 0.27991 cm. The thickness in the $[110]$ direction for specimen No. 2 was 0.25017 cm. For a discussion of uncertainties in thickness measurements, see Sec. 4.31.

Both diamonds were type I as shown by the presence of strong optical absorption around 8 microns wavelength. Most diamonds show a stress pattern between crossed Nicol prisms; these were no exception. Figure 2 shows the polarized light photographs through the polished (110) facets. X-ray reflection photographs showed the crystals to be single crystals.

A density of 3.512 g/cc was computed from known unit-cell dimensions as determined by x-rays.

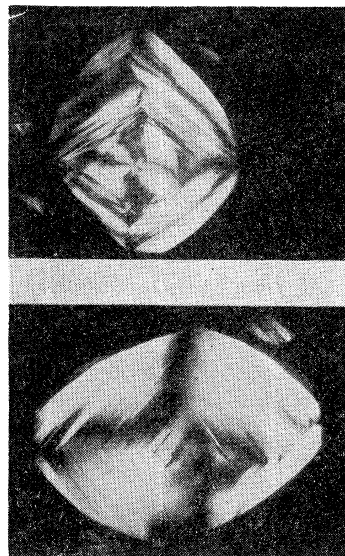


FIG. 2. Diamonds No. 1 (top) and No. 2 viewed through the (110) facets with crossed Nicol prisms.

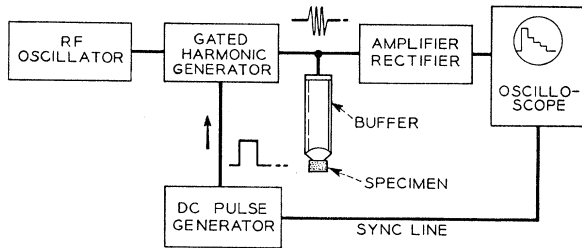


FIG. 3. Block diagram of circuit used for measuring velocities of propagation.

III. EXPERIMENTAL METHOD

3.1 Measurement of Velocities of Propagation for Ultrasonic Waves

For any crystalline material, plane waves may be propagated in an arbitrary direction with three possible velocities.⁴ Measurement of a sufficient number of velocities for different directions—along with the density—makes possible a determination of the adiabatic elastic moduli. Diamond, being cubic, requires three independent measurements. These were conveniently made by determining the velocities along the [110] direction. In addition (No. 1 crystal only), measurements for the [001] direction yielded c_{11} and c_{44} directly, and provided helpful cross checks.

Since the method used for determining velocities has been described previously, only a brief account will be given here. Figure 3 shows a block diagram of the circuit used. A repeated train of waves (long compared to the specimen delay, but less than the buffer round trip delay) is mainly reflected from the buffer-specimen interface, but partially transmitted within the specimen to give multiple reflections. At critical frequencies f_n , these waves are precisely in phase and give rise to a characteristic pattern on the oscilloscope. The velocity of propagation V is then given by

$$V = \frac{2tf_n}{n + \gamma/360}, \quad (3.1)$$

in which t is the specimen thickness, n is an integer representing very closely the number of wavelengths in $2t$, and γ is the phase angle in degrees associated with reflection of waves from the specimen-seal interface. Providing n is not too high (say <100), it is possible to determine n without ambiguity by measuring the frequency separation Δf between successive values of f_n . Then

$$n \cong f_n / \Delta f. \quad (3.2)$$

Because the specimens were so small, direct determination of γ was found to be impractical. Measurements were made at high enough frequencies, however, to make the phase shift at the specimen-seal interface very small compared with the total phase shift in the

⁴ For references see W. G. Cady, *Piezoelectricity* (McGraw-Hill Book Company, Inc., New York, 1946), p. 104.

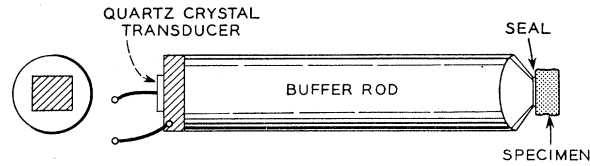


FIG. 4. Buffer unit for use at high frequencies.

specimen path. This matter will be treated more fully in a following section on possible errors.

Measurement over a frequency range—and extending to rather high frequencies—also made it possible to minimize dispersion errors due to diffraction effects⁵ and to energy reflected from the lateral boundaries. As will be evident from the data presented herein, use of frequencies in excess of 100 Mc/sec is indicated for satisfactory accuracies.

3.2 High Frequency Buffer Units

Figure 4 shows the type construction used for both shear and longitudinal waves. For the former, a 13-Mc Y-cut quartz plate was affixed to a fused silica rod $\frac{1}{2}$ in. in diameter and approximately 2 in. long. A standard silver-paste-solder seal was used, resulting in adequate bandwidths for harmonic operation up to at least 150 Mc/sec. A 30° bevel was cut on the “specimen” end to provide a $\frac{1}{8}$ in. \times $\frac{1}{8}$ in. working area having a 303 $\frac{1}{2}$ emery finish.

For longitudinal waves the buffer rod was of crystal-line quartz with length along the x axis. The 20 Mc/sec X-cut quartz transducer was oriented so that the Y and Z axes coincided for both transducer and buffer. (This construction allows cooling the unit to -200°C and below, if desired, without fracture of the components.)

3.3 Seal Materials for Attaching Specimens

For both longitudinal and shear waves, the specimens were attached to the active area of the buffer rods by means of a thin film of viscous liquid.⁶ For longitudinal waves, a light oil—Dow Corning DC703 pump oil—was also used.

3.4 rf Gate

Since it was essential that the rf gate used to produce the repeated train of waves close off completely between pulses, a harmonic generator circuit was used. Output from a stable continuous wave oscillator (variable in the range 8–12 Mc/sec) was multiplied in frequency by a series of harmonic generator stages turned on and off by a repeated dc pulse. The high-frequency output during the “off” period was quite free from leakage since the vacuum tube circuit elements were rendered

⁵ For the analogous case of diffraction effects for radiation into a liquid, refer to J. G. Parker, Naval Research Laboratory Report 4559 (unpublished).

⁶ Dow Corning resin, liquid 276-V9, blend 288 (poly- α -methylstyrene).

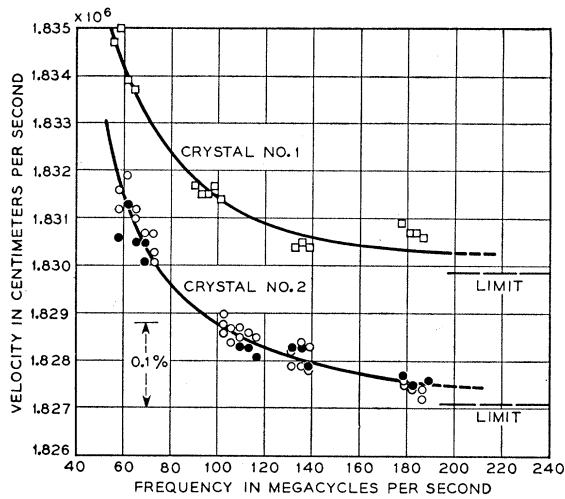


FIG. 5. Velocity in the [110] direction for longitudinal waves in diamond crystals No. 1 and No. 2.

completely passive by a high negative bias. Outputs up to 200 Mc/sec were readily obtained in this manner.

IV. RESULTS

4.1 Velocities of Propagation

Figures 5-8 show basic data for both crystals neglecting the effect of phase shift at the specimen-seal interface. For crystal No. 1, velocities for both the [110] and [001] directions are shown.

To provide an estimate of the phase angle γ [see Eq. (3.1)], calculations were made of the variation of γ with seal phase shift Bt . Results are shown by Fig. 9.

From previous experiments with the type of seal used, it was estimated that the seal thickness corresponded approximately to $Bt=50^\circ$ at 150 Mc/sec for shear waves.

Thus at this frequency $\gamma=2^\circ$; and for $n=60$ the velocity was corrected downward by 0.01%. Similar

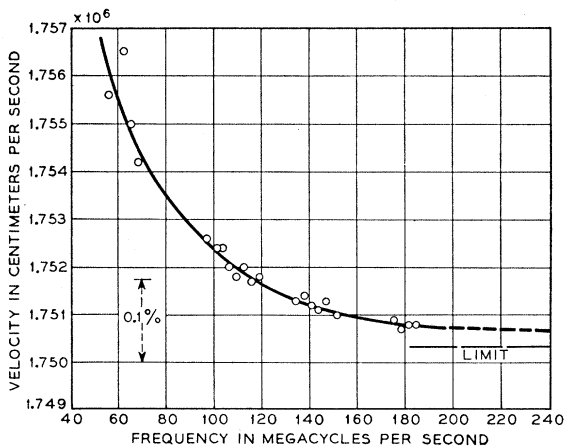


FIG. 6. Velocity in the [001] direction for longitudinal waves in diamond crystal No. 1.

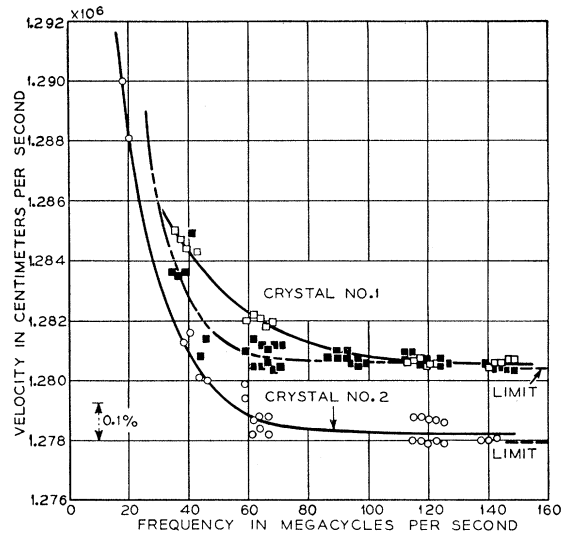


FIG. 7. Velocity of shear waves in diamond crystals No. 1 and No. 2. Open squares and circles—propagation in [110], particle motion in [001]; solid squares—propagation in [001].

correction at other frequencies and also for longitudinal waves was then possible.

The remaining excess was found to vary inversely as the square of the frequency, approximately. For a best fit to the data it was found that the limiting or "free space" velocity was only 0.01% less than the phase velocity at 150 Mc/sec (for shear waves).

Limiting velocity values obtained as described above are shown in Table I.

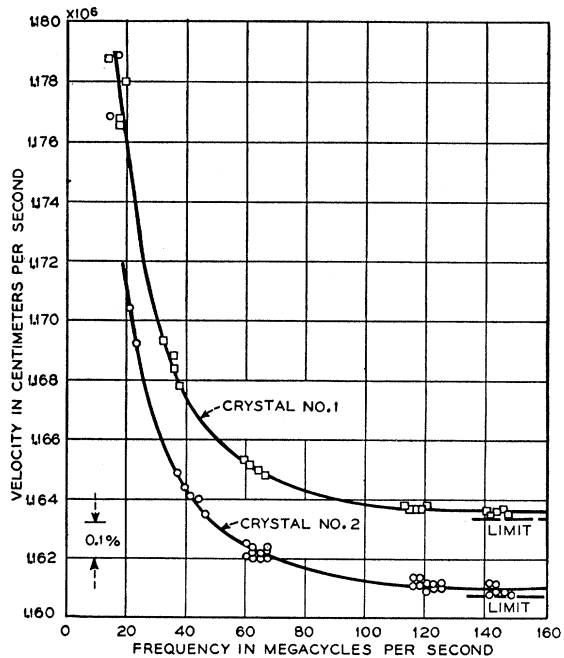


FIG. 8. Velocity of shear waves in diamond crystals No. 1 and No. 2 for propagation in [110] direction with particle motion in [110] direction.

TABLE I. Velocities of propagation for diamond.

Specimen	Direction of propagation	Direction of particle motion	Type of mode	Equation for velocity	Velocity at 27°C in cm/sec
Crystal No. 1	110	$\bar{1}\bar{1}0$	Shear	$[(0.5c_{11}-0.5c_{12})/\rho]^{\frac{1}{2}}$	1.1634×10^6
	110	001	Shear	$(c_{44}/\rho)^{\frac{1}{2}}$	1.2804×10^6
	110	110	Long.	$[(0.5c_{11}+0.5c_{12}+c_{44})/\rho]^{\frac{1}{2}}$	1.8299×10^6
	001	001	Long.	$(c_{11}/\rho)^{\frac{1}{2}}$	1.7503×10^6
	001	...	Shear	$(c_{44}/\rho)^{\frac{1}{2}}$	1.2804×10^6
Crystal No. 2	110	$\bar{1}\bar{1}0$	Shear	(see above)	1.1608×10^6
	110	001	Shear	(see above)	1.2780×10^6
	110	110	Long.	(see above)	1.8271×10^6

4.2 Elastic Moduli

From the values of velocity of propagation listed in Table I the adiabatic elastic moduli were computed; they are listed in Table II. For Crystal No. 1 the cross-checks on c_{11} and c_{44} are even better than anticipated.

For all calculations, a density of 3.512 g/cc was used. (See Sec. II.)

4.3 Discussion of Uncertainties

4.31 Length Measurement and Taper

The uncertainty in length (averaged over the specimen face) is estimated to be $\pm 0.02\%$. This corresponds to estimating to the nearest 0.2 division (1 division = 0.1 mil) on the Sheffield gauge used. The taper for the (110) faces and the (001) faces of Crystal No. 1 was less than 1.5 minutes. The effective path length for a distance of travel represented by 20 pulses (this corresponds approximately to actual measurement conditions) was computed to be within 0.01% of the path length based on the average thickness figure used. The value of 0.04% listed in Table III is therefore amply conservative.

For the No 2 diamond, however, the taper of approximately 5 minutes could be responsible for perhaps as much as 0.07% error. Correction for this would bring the velocity data into better agreement with that for specimen No. 1.

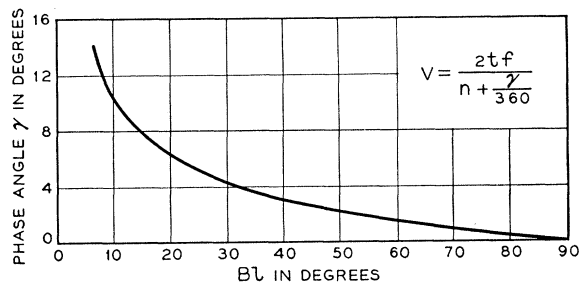


FIG. 9. Phase angle γ versus seal phase shift Bl —based on shear wave characteristic impedances as follows: 8.28×10^6 for fused silica buffer, 0.9×10^6 for seal, 40.6×10^6 for diamond.

4.32 Frequency

The frequency corresponding to a given oscilloscope pattern was reproducible to within $\pm 0.015\%$. Maximum error in absolute frequency measurement was ± 500 cps in 10^7 or $\pm 0.005\%$, making the total uncertainty 0.02%.

4.33 Dispersion

An uncertainty of $\pm 0.01\%$ has been allowed for dispersion effects. This is equal to the correction applied at the highest frequency used.

4.34 Coupling Seal

Although it seems unlikely that for a properly formed seal the uncertainty (after correction for phase shift) would be greater than 0.01%, it was found that velocities varied as much as $\pm 0.04\%$ as a function of seal reproducibility. This was probably due to a non-uniform thickness of the seal, with consequent refraction of the beam.

4.35 Temperature

Measurements were made at $27^\circ\text{C} \pm 2$. Velocity variations within this range were less than 0.01%.

4.36 Orientation

Errors in crystal orientation ranged from 8 minutes to $1^\circ 15'$ for the three sets of measurements made. Errors due to this source were calculated to be less than 0.02%.

TABLE II. Adiabatic elastic moduli for diamond at 27°C.^a

Modulus	No. 1	No. 2	Remarks
c_{11}	$10.756 \pm 0.63\%$	10.720	Data for [110]
	$10.759 \pm 0.30\%$...	Data for [001]
c_{12}	$1.249 \pm 5.4\%$	1.256	Data for [110]
	$1.252 \pm 4.9\%$...	(Data for [001] and
	$1.245 \pm 11.0\%$...	[110] combined)
c_{44}	$5.758 \pm 0.30\%$	5.736	Data for [110]
	$5.758 \pm 0.30\%$...	Data for [001]

^a Values are based on a density of 3.512 g/cc. Values are in units of 10^{12} dynes/cm².

TABLE III. Estimated maximum uncertainties for velocities.

Length	0.04%
Frequency	0.02%
Dispersion	0.01%
Seal coupling	0.05%
Orientation	0.02%
Temperature variations	0.01%
Total 0.15%	

4.37 Total Uncertainty for Velocity

As shown by Table III, a *maximum* uncertainty of 0.15% could exist for any one velocity. Probable uncertainties would be less than this amount, as perhaps is evidenced by the excellent cross check for Crystal No. 1.

4.38 Maximum Uncertainties for Elastic Moduli

The limits listed in Table II are based on the conservative assumption that all errors in velocities add in the same direction so as to maximize the uncertainties for the elastic moduli.

Because the absolute value of c_{12} is quite low, relatively large fractional uncertainties are possible. On the other hand, a comparison of values for c_{12} obtained from different combinations of data indicates no such large disagreement.

V. COMPARISON OF PRESENT WORK WITH THAT OF OTHERS

5.1 Elastic Moduli

Table IV shows a comparison of elastic moduli with those obtained by Bhagavantam and Bhimasenachar¹ and by Prince and Wooster.² Large disagreement is to be noted for c_{44} and c_{12} , particularly the latter.

Bhagavantam does not discuss errors involved in the "wedge" method as used for measurements on diamond, except to note that frequency reproducibility is of the order of 1 or 2%.^{7,8} It is claimed, however, that "the method is, on the whole, capable of giving elastic constants accurate to about 5%." However, the choice of propagation directions used determines to a large extent the magnitude of uncertainties. For example, Bhagavantam obtains data with two orientations, namely [111] and [110]. As a result, if errors in velocity are assumed to maximize errors in elastic moduli, uncertainties as high as 20% could exist (corresponding to 1% errors in velocity).

In addition, since only two velocity relations accrue from propagation in the [111] direction, a great deal of weight must be attached to the one longitudinal wave measurement reported for [110].

Another point to be considered in connection with the ultimate accuracy of the "wedge" method is the

⁷ S. Bhagavantam and J. Bhimasenachar, Proc. Indian Acad. Sci. **20**, 298 (1944).

⁸ S. Bhagavantam, Proc. Indian Acad. Sci. **41**, 72 (1955).

TABLE IV. Comparison of results.^a

Modulus	Present work	Bhagavantam and Bhimasenachar	Prince and Wooster
c_{11}	10.76	9.5	11.0
c_{12}	1.25	3.9	3.3
c_{44}	5.76	4.3	4.4
$k = \frac{1}{3}(c_{11} + 2c_{12})$	4.42	5.8	5.9

^a Values are in units of 10^{12} dynes/cm².

effect of coupling between wedge and specimen, and of course dispersion effects in general.

5.2 Volume Compressibility

Adams⁹ and Williamson¹⁰ have reported isothermal compressibilities corresponding to a bulk modulus of 6.3 and 5.6 (units of 10^{12} dynes/cm²), respectively. These values may be compared with those listed in Table IV.

5.3 Thermal Scattering of Light in Diamond

Chandrasekharan¹¹ has reported measurements of the Doppler shifts for the scattered spectrum, using $\lambda_{2536.5}$ mercury radiation. His results indicate that the two shear wave velocities (say, along [110]) must be much closer to each other than indicated by Bhagavantam's elastic moduli, since only one pair of distinct lines corresponding to shear waves was observed. Also, the measured shift (shear component) was "definitely larger" than calculated. The present work may be consistent with these findings, since the shear velocities along [110] are both larger in magnitude and more nearly equal to each other than obtained from Bhagavantam's values.

5.4 Theoretical Calculations

Krishnamurti¹² has evaluated the elastic moduli of diamond on a theoretical basis using atomic force constants. His results agree well with Bhagavantam's data. On the other hand, Born¹³ discusses an extended theory that is not substantiated by Bhagavantam's data. The values of this report do not appear to fit Born's relation of elastic moduli, either.

VI. CONCLUSIONS

1. Measurements involving three sets of wave velocities in two high quality single crystals of diamond have resulted in values of elastic moduli differing appreciably from those previously reported. Specifi-

⁹ L. H. Adams, J. Wash. Acad. Sci. **11**, 45 (1921).

¹⁰ E. D. Williamson, J. Franklin Inst. **193**, 491 (1922).

¹¹ V. Chandrasekharan, Proc. Indian Acad. Sci. **A32**, 379 (1950).

¹² K. Krishnamurti, Proc. Indian Acad. Sci. **A33**, 325 (1951).

¹³ M. Born, Nature **157**, 582 (1946).

cally, c_{12} is much lower and c_{44} is much higher than literature values. General agreement for c_{11} exists.

2. The data obtained were remarkably self-consistent, particularly for the two directions of propagation in Crystal No. 1 ([110], [001]).

3. Measurements made on small crystals (thickness and lateral dimensions ~ 2.5 – 3.0 mm) should extend

into the 100–200 Mc/sec range to minimize errors due to seal coupling and dispersion.

VII. ACKNOWLEDGMENT

Appreciation is here expressed to T. B. Bateman for making many of the measurements reported in this paper.

PHYSICAL REVIEW

VOLUME 105, NUMBER 1

JANUARY 1, 1957

Acoustic Relaxation Effect in Mn_3O_4 †

M. E. FINE AND CHARLES CHIOU

Department of Metallurgy, Northwestern Technological Institute, Evanston, Illinois

(Received July 23, 1956)

Internal friction effects occur in Mn_3O_4 which have been attributed to stress-induced change in the distribution of Mn^{++} and Mn^{+++} . The activation energy is 0.4 ev per unit of process responsible for the internal friction.

IF the internal friction of hausmannite, nominal composition Mn_3O_4 , is plotted as a function of temperature, peaks at particular temperatures are observed. By analogy with magnetite and Ni-Fe ferrites which are isomorphous with Mn_3O_4 and in which similar effects occur,¹ the internal friction peaks in Mn_3O_4 have been attributed to a stress-induced change in the distribution of Mn^{++} and Mn^{+++} .

EXPERIMENTAL PROCEDURE AND DATA

Sample polycrystalline rods of Mn_3O_4 were prepared by slowly heating powdered $MnCO_3$ in air to $1100^\circ C$ and holding for one day. The product was powdered, pressed into rods using a wax binder, and then sintered at 1100 to $1200^\circ C$ in helium or air. Each sample was examined by x-rays; no other phases besides Mn_3O_4 were detected. After sintering the apparent densities varied from 77 to 91% of the true value for Mn_3O_4 (4.89 g/cm³, calculated from the lattice constants²). Internal friction and Young's modulus were determined as functions of temperature by the resonant longitudinal vibration method using piezoelectric excitation and detection of vibrations.^{3,4} Red sealing wax or zinc phosphate dental cement were used to cement the crystal to the Mn_3O_4 rod. The frequencies varied from 50 to 180 kc/sec, the strain amplitudes were in the 10^{-7} – 10^{-8} range.

The first specimen studied was sintered in air at

$1200^\circ C$. With vibrations of 60 kc/sec, the fundamental resonant frequency, an internal friction peak occurs near $75^\circ C$ (Fig. 1). With 180-kc/sec vibrations the peak occurs near $105^\circ C$ (Fig. 1). The shift in temperature of the peak corresponds to an activation energy of 9500 cal per mole or 0.4 ev per unit of process responsible for the internal friction.

The second specimen was sintered in He at $1100^\circ C$. An internal friction peak occurs near $-10^\circ C$ (Fig. 2, Curve A). The specimen was subsequently sintered at $1200^\circ C$ in air; a second internal friction peak near $75^\circ C$ is observed (Fig. 2, Curve B).

In Fig. 3, Young's modulus is plotted as a function of temperature for the first specimen. As expected, Young's modulus decreases rapidly on heating in the region of the internal friction peak since the effective modulus varies from the unrelaxed to the relaxed value.

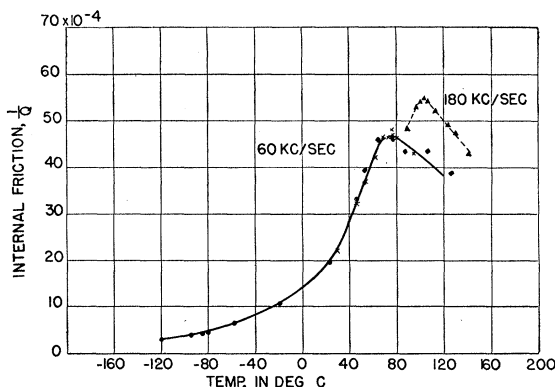


FIG. 1. Internal friction of Mn_3O_4 , sample 1. Sintering Treatment: Four days at $1100^\circ C$ in air, then two days at $1200^\circ C$ in air. Apparent density, 91%; \blacktriangle \blacklozenge dental cement joint; \bullet red sealing wax joint.

† This research was supported in part by the U. S. Air Force through the Air Force Office of Scientific Research of the Air Research and Development Command.

¹ M. E. Fine and N. T. Kenny, *Phys. Rev.* **94**, 1573 (1954); **96**, 1487 (1954).

² F. C. Romeijn, *Philips Research Repts.* **8**, 319 (1953).

³ L. Balamuth, *Phys. Rev.* **45**, 715 (1934).

⁴ M. E. Fine, *Rev. Sci. Instr.* **25**, 1188 (1954).

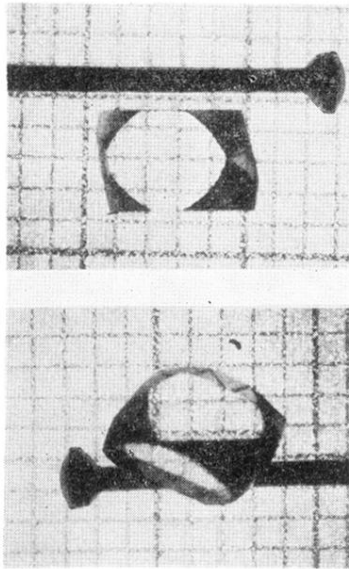


FIG. 1. Diamond No. 1 on millimeter paper background with common straight pin for comparison.

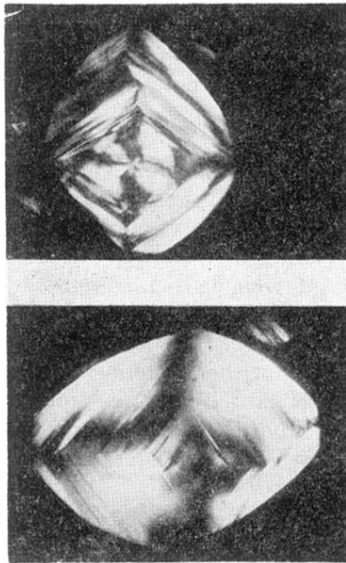


FIG. 2. Diamonds No. 1 (top) and No. 2 viewed through the (110) facets with crossed Nicol prisms.